

Normal ferroelectric to ferroelectric relaxor conversion in fluorinated polymers and the relaxor dynamics

SHIHAI ZHANG^{*†}, ROB J. KLEIN, KAILIANG REN, BAOJIN CHU, XI ZHANG, JAMES RUNT

Materials Research Institute, The Pennsylvania State University, University Park, PA 16802, USA
E-mail: zhangs@research.ge.com

Q. M. ZHANG

Materials Research Institute, The Pennsylvania State University, University Park, PA 16802, USA; Department of Materials Science and Engineering, The Pennsylvania State University, University Park, PA 16802, USA; Department of Electrical Engineering, The Pennsylvania State University, University Park, PA 16802, USA

To elucidate the molecular origin of the polarization dynamics in the ferroelectric relaxor poly(vinylidene fluoride–trifluoroethylene-chlorofluoroethylene) (P(VDF-TrFE-CFE)) terpolymer, a broadband dielectric study was carried out in the frequency range from 0.01 Hz to 10 MHz and temperatures from -150°C to 120°C for the terpolymer and a normal ferroelectric P(VDF-TrFE) copolymer. The relaxation processes were also studied using dynamic mechanical analysis. It was shown that in the terpolymer, which was completely converted to a ferroelectric relaxor, there is no sign of the relaxation process associated with the ferroelectric-paraelectric transition which occurs in the P(VDF-TrFE) copolymer. In the copolymer, three additional relaxation processes have been observed. It was found that the relaxation process β_a , which was commonly believed to be associated with the glass transition in the amorphous phase, in fact, contains significant contribution from chain segment motions such as domain boundary motions in the crystalline region. In the temperature range studied, the terpolymer exhibits the latter three relaxation processes with the one (termed β_r) near the temperature range of β_a significantly enhanced. This is consistent with the observation that in conversion from the normal ferroelectric to a ferroelectric relaxor, the macro-polar domains are replaced by nano-polar-clusters and the boundary motions as well as the reorientation of these nano-clusters generate the high dielectric response. The experimental data also reveal a broad relaxation time distribution related for the β_r process whose distribution width increases with reduced temperature, reflecting the molecular level heterogeneity in the crystalline phase due to the random introduction of the CFE monomer in the otherwise ordered macro-polar domains. The random interaction among the nano-clusters as well as the presence of the random fields produces ferroelectric relaxor behavior in the terpolymer.

© 2006 Springer Science + Business Media, Inc.

*Author to whom all correspondence should be addressed.

†Present Address: GE Global Research, Niskayuna, NY 12304, USA.

0022-2461 © 2006 Springer Science + Business Media, Inc.

DOI: 10.1007/s10853-006-6081-2

1. Introduction

In the last several decades, poly(vinylidene fluoride) (PVDF) and its copolymer with trifluoroethylene (P(VDF-TrFE)) have been studied extensively for their ferroelectric and electromechanical properties [1–4]. Recently, it was discovered that by proper defect modifications, the normal ferroelectric P(VDF-TrFE) copolymer can be converted to a relaxor ferroelectric polymer, which is the first and only known ferroelectric polymer relaxor [5, 6]. Interestingly, the relaxor ferroelectric polymers exhibit large electrostriction and high room temperature dielectric constant, which are attractive for a broad range of applications such as acoustic transducers, microactuators in MEMS, and electro-optic devices. These advances indicate the great potential of polymeric materials for achieving high functional responses compared with their inorganic counterparts, as well as the great need to understand the molecular origins of these responses.

For high energy electron irradiated P(VDF-TrFE) copolymers, it was established that the defects introduced by the irradiation break up the macroscopic polar-domains, leading to the conversion to the ferroelectric relaxor [5, 7, 8]. Analogously, in the terpolymer of poly(vinylidene fluoride-trifluoroethylene-1,1-chlorofluoroethylene) (P(VDF-TrFE-CFE)), the bulky termonomer CFE units serve as local defects to the polarization ordering in the crystalline regions, which convert the all-trans polar-conformation to a phase with a mixture of trans-gauche (TG₃TG'), all-trans and TG₃TG₃' conformations, which is macroscopically non-polar and exhibits ferroelectric relaxor behavior [9–17]. Under external electric field, both the local polar-region reorientation and the induced local conformation change result in large macroscopic electrostriction [11, 17]. For example, for a P(VDF-TrFE-CFE) terpolymer with certain composition, it was observed that a thickness strain of higher than -7% and transverse strain of 5% can be achieved [17].

While the microstructure and electromechanical properties of these polymers have been investigated in the past, the molecular origins of different dielectric relaxation processes, some of which contribute to the ferroelectric relaxor response of the polymer, are not clearly understood [18–22]. These relaxations reflect the molecular motions in both crystalline and amorphous phases and are also closely related to the macroscopic electromechanical response. In this paper, we report a detailed study on the broadband dielectric spectra of a ferroelectric relaxor P(VDF-TrFE-CFE) terpolymer with different thermal histories and electrical poling history, with the aim to explore the relaxor dynamics and their molecular origins. To gain more insight into the dynamics of the terpolymer, the polarization dynamics of the parent P(VDF-TrFE) copolymer was also studied under similar conditions.

2. Experimental

2.1. Sample preparation

A P(VDF-TrFE) copolymer with VDF content of 68 mol% was used in this study and it has a weight-average molecular weight (M_w) of 367,000 and a polydispersity of 2.7. P(VDF-TrFE-CFE) with VDF/TrFE/CFE molar ratio of 63/37/7.5 was synthesized via suspension polymerization using an oxygen-activated initiator (For easy comparison with the P(VDF/TrFE) copolymer, we use VDF_{*x*}/TrFE_{*1-x*}/CFE_{*y*} to describe the composition of the terpolymer, where $x/(1-x)$ is the VDF/TrFE mole ratio and y is the mol% of CFE in the terpolymer) [9]. The terpolymer has a M_w of 670,000 and M_n of 238,000. Molecular weights were determined by gel permeation chromatography using narrow molecular weight polystyrene as standards and tetrahydrofuran as the mobile phase. These two compositions were selected since they have similar VDF/TrFE ratio.

Polymer films with thickness around 20 μm were prepared by solution casting with dimethylformamide (DMF) as the solvent. The samples were annealed in a vacuum oven overnight, at 120°C for terpolymer and 140°C for copolymer, to enhance their crystallinity. Quenched samples were obtained by melting the above films and then cooling to room temperature within 5 s. For electrical characterization, a 40 nm layer of gold was sputtered on both sides of the film.

2.2. Characterization

DSC measurements were carried out with a TA Q100 instrument at a heating rate of 10°C/min, with sample weights around 5 mg. IR spectra were recorded using a Nicolet FT-IR spectrometer with 64 scans averaged at a resolution of 2 cm^{-1} . Wide angle X-ray diffraction (WAXD) studies were performed using a Scintag Cu-K α diffractometer with an X-ray wavelength of 1.54 Å. Polarization hysteresis loops at room temperature were collected using a Sawyer-Tower circuit with a frequency of 10 Hz.

Isothermal dielectric spectra $\varepsilon^*(f, T)$ were collected using a Novocontrol GmbH Concept 40 broadband spectrometer in the frequency domain (10 MHz to 0.01 Hz). The AC voltage for weak field dielectric measurement is 1.5 V. The temperature was controlled by a Novocontrol Quatro Cryosystem with stability better than $\pm 0.1^\circ\text{C}$. Data collection did not start until the temperature had been stabilized at least 10 min. To better reveal details of the dynamics, the isothermal data at different temperatures were reorganized and the dielectric spectra at constant frequency as a function of temperature were plotted, that is, isochronal presentation.

Dynamic mechanical analysis (DMA) was performed with a TA DMA 2980 instrument in the step-scan mode

at frequencies from 20 to 0.1 Hz. Samples for DMA were $\sim 200 \mu\text{m}$ thick.

3. Results and discussions

3.1. Property comparison between the normal ferroelectric P(VDF-TrFE) copolymer and the ferroelectric relaxor P(VDF-TrFE-CFE) terpolymer

To provide some background, we will first review the experimental data related to the conversion from the normal ferroelectric phase of the P(VDF-TrFE) copolymer to the ferroelectric relaxor character of the P(VDF-TrFE-CFE) terpolymer.

Presented in Figs 1 and 2 are a comparison of the polarization and dielectric (real part) responses of the copolymer and terpolymer. As a ferroelectric, the copolymer exhibits a nearly square polarization hysteresis loop due to the large nucleation barrier for domain wall motion. The remnant polarization (P_r) is 75 mC/m^2 and the cohesive electric field (E_c) is around 60 MV/m . This hysteresis is nearly eliminated in the P(VDF-TrFE-CFE) terpolymer, as expected for a relaxor ferroelectric at temperatures near the dielectric constant maximum (due to the absence of macroscopic polarization domains). P_r and E_c for the relaxor terpolymer are much smaller, i.e., 2.5 mC/m^2 and 4 MV/m , respectively. For the dielectric constant, the P(VDF-TrFE) copolymer exhibits a sharp ferroelectric-paraelectric (F-P) transition at 110°C (see Fig. 2) and the peak position does not depend on frequency. In contrast, the P(VDF-TrFE-CFE) terpolymer shows a much broad peak in the dielectric constant near room temperature and the peak position shifts progressively to higher temperature with frequency, which is a feature typical of ferroelectric relaxors [23]. It should be noted that at some temperatures below the dielectric constant maximum, the relaxor polymer exhibits large polarization hysteresis, which is another characteristic of ferroelectric relaxors [5, 24].

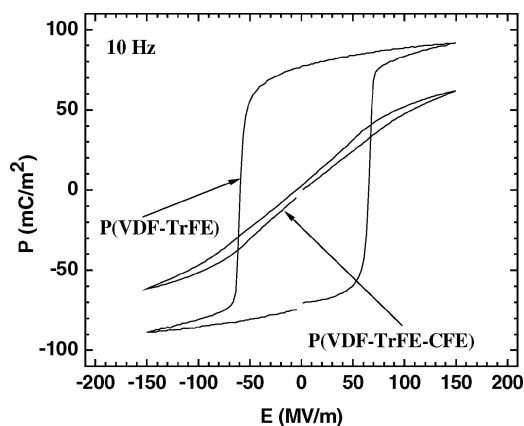


Figure 1 Polarization hysteresis loop measured at room temperature using 10 Hz triangular voltage signal.

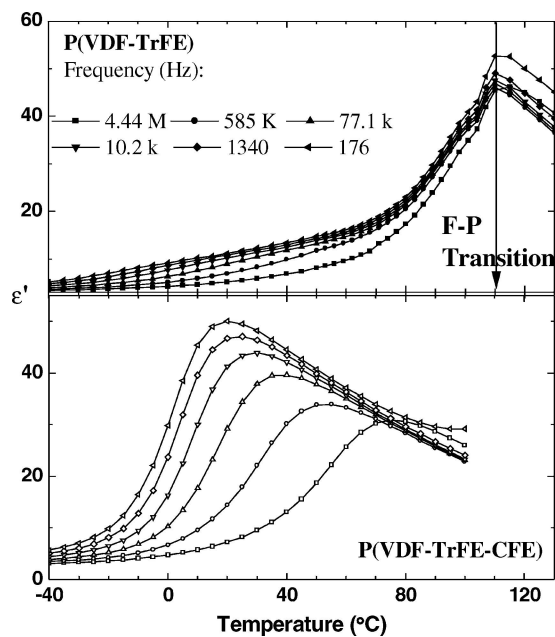


Figure 2 Comparison of the dielectric spectra of the normal ferroelectric P(VDF-TrFE) and ferroelectric relaxor P(VDF-TrFE-CFE).

The conversion from the normal ferroelectric polymer to a ferroelectric relaxor is also reflected by molecular conformation changes in the polymer. In ferroelectric copolymers, a majority of the crystallite chains ($\sim 75\%$ for 68/32 composition) are in the polar *all trans* conformation, leading to a high effective dipole moment. In contrast, the majority of the P(VDF-TrFE-CFE) terpolymer crystallite chains adopt non-polar conformations, as a result of the defects introduced by the bulky CFE monomer units. The different chain conformations associated with the crystalline phases can be distinguished by their characteristic bands in FTIR spectra, which are presented in Fig. 3. The bands at 1290 cm^{-1} and 850 cm^{-1}

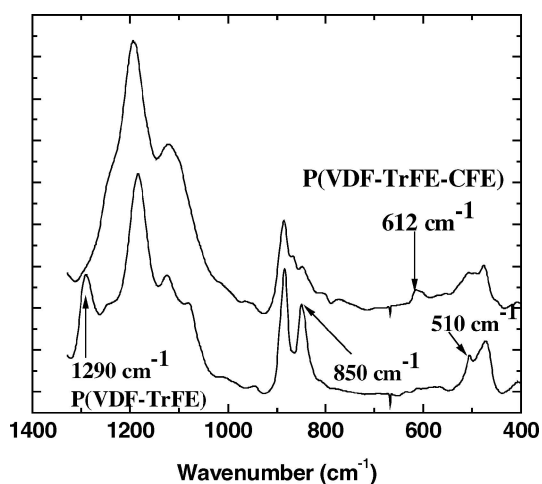


Figure 3 FTIR spectra (absorbance) at room temperature. The spectrum of the terpolymer is shifted vertically.

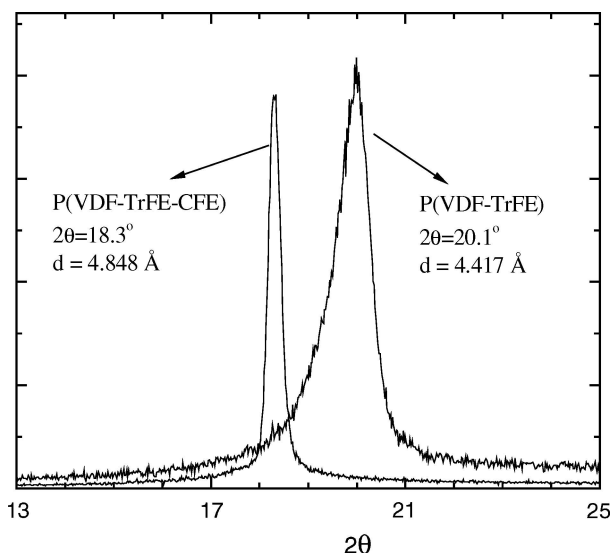


Figure 4 Wide angle X-ray diffraction data in the (110, 200) reflection region. Wavelength used is 1.54 Å (Cu-K α).

represent the *all trans* conformation [25] and they exhibit large absorbances in the spectrum of the copolymer, but significantly reduced in the relaxor terpolymer. The band at 612 cm^{-1} corresponds to the TGTG' conformation and it can only be observed in the spectrum of the terpolymer. The absorbance at 510 cm^{-1} represents the C-F bending mode in the polar T_3GT_3G' conformation and it is observed in both spectra. From the FTIR data, it can be deduced that $\sim 55\%$ of the terpolymer chains exhibit TGTG' non-polar conformations, while only 20% of the chains are in the all-trans polar conformation.

The ferroelectric crystallites in the copolymer are transformed to nonpolar crystallites in the terpolymer after introducing the CFE defects. This is also evident in their corresponding X-ray diffraction patterns provided in Fig. 4. The ferroelectric P(VDF-TrFE) copolymer displays a

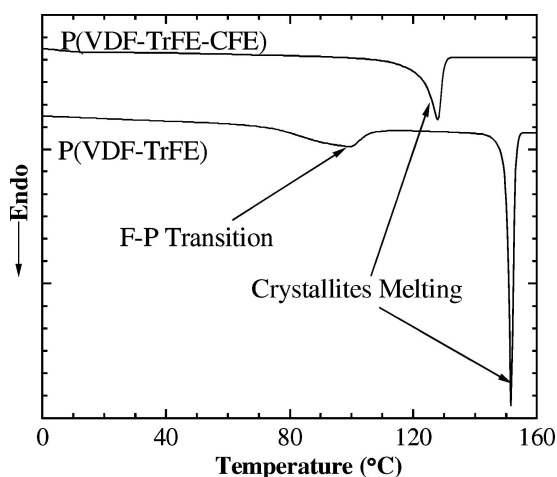


Figure 5 DSC traces of copolymer and terpolymer. Heating rate is 10°C/min.

diffraction peak at $2\theta = 20.1^\circ$ (originating from the (110, 200) reflection and corresponding to a lattice spacing of 4.417 Å in ferroelectric crystalline phases). This peak shifts to lower diffraction angle (18.3°) for the P(VDF-TrFE-CFE) terpolymer, indicating a larger lattice spacing of 4.848 Å (from the (110, 200) reflection in nonpolar crystallites) [11, 15]. The non-polar nature of the terpolymer crystallites is also supported by the disappearance of the F-P transition in the DSC thermogram, compared with the strong ferroelectric-paraelectric transition exhibited by ferroelectric P(VDF-TrFE) copolymers ($\sim 100^\circ\text{C}$ for the 68/32 composition, Fig. 5).

3.2. Dynamics of the normal ferroelectric P(VDF-TrFE) copolymer

To facilitate an understanding of the dielectric dynamics in the ferroelectric relaxor terpolymers, the dynamics of the normal ferroelectric copolymer [25–27] having a similar VDF/TrFE ratio was investigated initially. Fig. 6 presents dielectric spectra (measured during the heating run) for the P(VDF-TrFE) copolymer in the temperature range from -60 to 140°C . Dielectric data acquired at temperatures from -150 to -60°C will be presented later. In the temperature range from -150 to 140°C , four dielectric relaxation processes can be identified. As has been pointed out earlier, the peak in the dielectric constant at 110°C corresponds to the F-P transition. In the DSC thermogram, the same process is also observed as an endotherm with $\Delta H = 25$ J/g. Reflecting its first-order phase transition nature, a large thermal hysteresis is observed and the

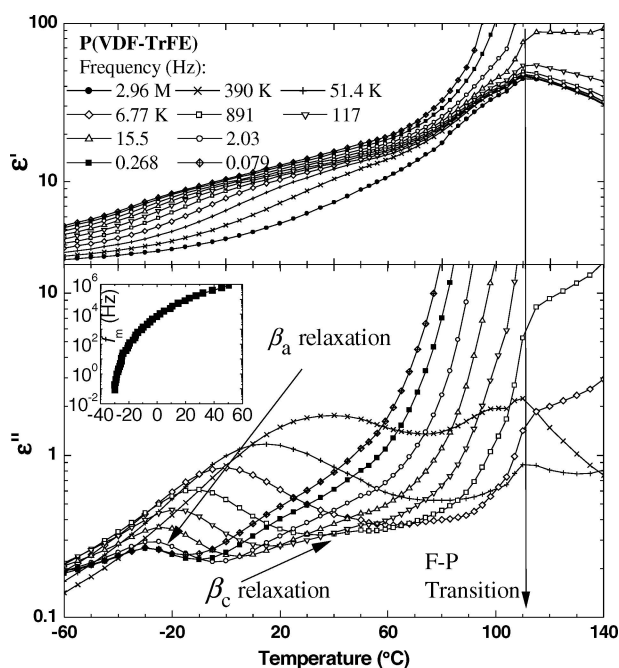


Figure 6 Dielectric spectra of P(VDF-TrFE) copolymer. Inset: peak locations of the β_a relaxation taken from the ϵ'' spectra.

reverse transition during cooling occurs at a temperature 50°C lower than that measured on heating.

Two frequency-dependent processes are visible (particularly in the loss spectra) around room temperature in Fig. 6. The process at lower temperatures (located at 0°C at 10.2 kHz) is relatively strong and has been traditionally assigned to the dynamic glass transition of segments in the amorphous portion of the copolymer (denoted as β_a hereafter) [28, 29]. However, a recent study by Omote and coworkers found that this process is also present in ‘single crystalline’ P(VDF-TrFE), although with slightly lower intensity [30]. Since there is essentially no amorphous phase in the single crystalline polymer, it was proposed that this process may also reflect chain motions due to structural defects in the crystalline phase. As demonstrated later, this dielectric relaxation includes a significant contribution from domain wall and polar defect motions in the normal ferroelectric P(VDF-TrFE) copolymer.

The β_a anomaly shifts to higher temperatures with increasing frequency, reflecting the speeding up of polymer chain motions with temperature. Its temperature-frequency relationship is usually modeled with the Vogel-Fulcher (VF) law $f_m = f_0 \times \exp[-U/k(T-T_0)]$ (inset in Fig. 6) [31], where f_m represents the average relaxation frequency, U is a constant, and T_0 is the Vogel temperature at which the relaxation process becomes frozen. Fitting the data in Fig. 6 leads to the following fitting parameters: $f_0 = 253$ MHz, $U = 5.55$ kJ/mol = 0.0575 eV, and $T_0 = 209.0$ K. It should be emphasized that to precisely determine the parameters in the VF equation, very reliable f_m data at temperatures close to T_0 , or at least close to the glass transition temperature T_g ($T_g \approx T_0 + 30 \sim 50^\circ\text{C}$) are required, which necessitate long time data acquisition (i.e., the dielectric constant measured at near static conditions). Fitting the VF law without sufficient experimental data can generate significantly different f_0 , U ,

and T_0 values. This readily explains the scattered fitting results in the literatures [5, 7, 18, 21]. The dipole reorientation associated with the β_a process leads to a moderate increase in the relaxation strength $\Delta\epsilon$ (defined as $\epsilon'[\text{high temperature}] - \epsilon'[\text{low temperature}] \sim 9.5$ at 1 kHz, significantly smaller than that at the F-P transition. However, $\Delta\epsilon$ is typically 3~5 for the segmental (glass) transition in other completely amorphous polymers [32], much smaller than that observed for the β_a process in P(VDF-TrFE) (particularly considering that it contains only ~25% amorphous segments). The large $\Delta\epsilon$ for β_a , however, is consistent with the scenario that the domain wall and other polar-defect motions in the crystalline phase contribute significantly to the observed dielectric β_a relaxation process.

While the above two dielectric anomalies, i.e., the F-P transition of the crystalline phase and the complex β_a relaxation, have been reported in many studies [25–29], a third process, taking place at slightly higher temperature than the β_a process, can only be observed in low-frequency dielectric spectra. Although the nature of this process (referred to as β_c) is still under debate, most results support its origin in the crystallite/amorphous interface [33]. β_c is significantly weaker than β_a in the dielectric spectra, and they apparently merge into one process at frequencies above 10 kHz.

The β_c process is also observed in the DMA spectrum (Fig. 7) where it is more prominent than the β_a process. Furthermore, the relative f - T locations of the β_a process in DMA and dielectric spectra depend on the manner in which they are defined. In loss spectra ($\tan \delta = \epsilon''/\epsilon'$ or E''/E'), the mechanical relaxation is about one decade slower than the comparable dielectric process (Fig. 8). This behavior is reasonable since the slowest (and

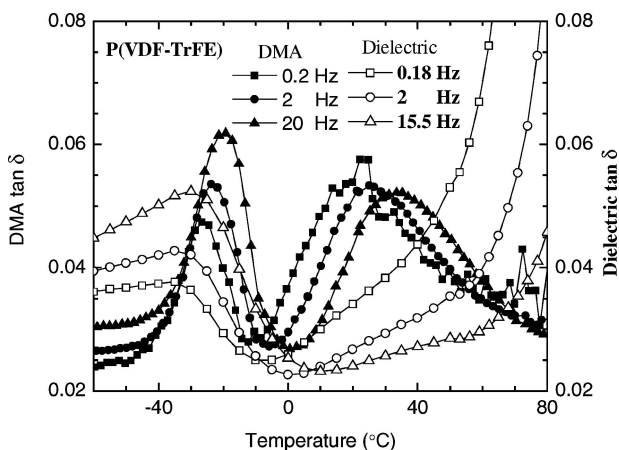


Figure 7 Comparison of the dielectric and DMA spectra of P(VDF-TrFE) copolymer. The β_c relaxation can be clearly identified in the DMA spectra.

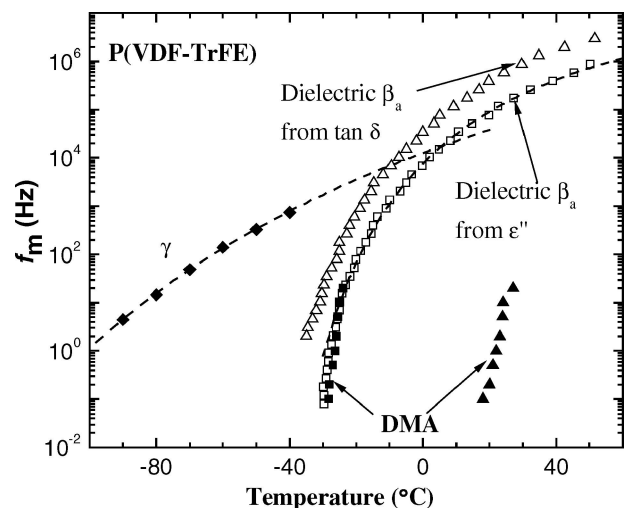


Figure 8 Relaxation time-temperature map of P(VDF-TrFE) copolymer. Data for the γ relaxation are curve fitting results from the isothermal spectra. Other data are directly read from the isochronal spectra. Dashed lines represent the VF-law and Arrhenius fitting to the experimental data.

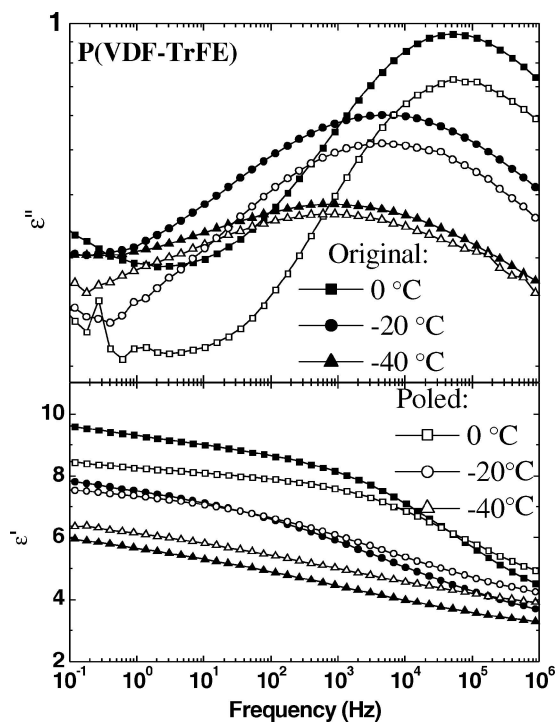


Figure 9 Poling effect on the β_a relaxation of the P(VDF-TrFE) copolymer. Samples were poled at 100 MV/m at 50°C for 10 min.

largest) chain segments carry most mechanical stress and determine the average relaxation time in DMA, whereas the dielectric relaxation time is simply a weight-average quantity.

To further explore the molecular origin of the β_a dielectric process in P(VDF-TrFE), electric poling experiments were performed. In normal ferroelectric materials, electrical poling usually improves the polar-ordering in the crystalline region and reduces the domain wall density, and so dielectric dispersion originating from domain wall motion should be weakened [23, 24]. After poling at 100 MV/m at 50°C for 10 min, the F-P transition of the copolymer is clearly sharpened due to the formation of larger polarization domains. The β_a process, however, is weakened considerably after poling (Fig. 9), and its location shifts to slightly higher frequencies compared with the unpoled samples. The low-frequency dielectric constant in the glass transition region also decreases after poling. Since a poling field of 100 MV/m at 50°C will not have a marked effect on the crystallinity (converting amorphous chain segments into crystallites), the decrease in strength of the β_a process is attributed to reduction in the density of domain wall and other defects in the crystalline phase due to poling. The result is consistent with the scenario that there is a quite significant contribution to the β_a process from the domain walls and other defects in the crystalline phase.

A dielectric study was also performed on copolymer samples quenched from the melt. This leads to a reduc-

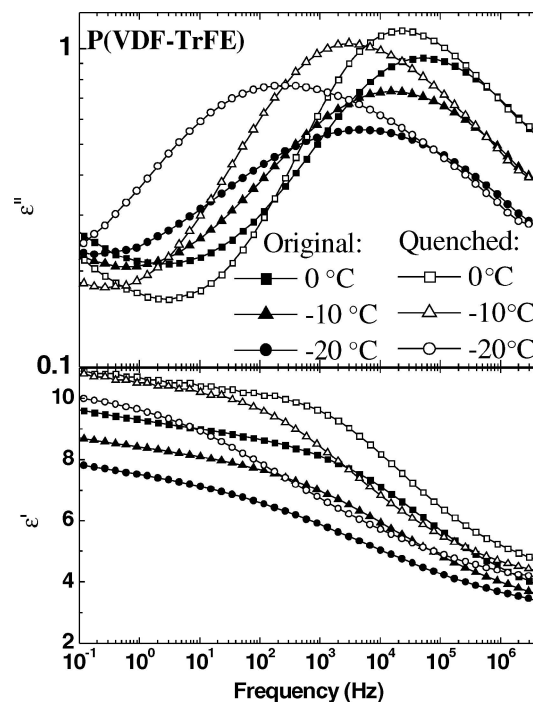


Figure 10 Isothermal dielectric spectra of quenched P(VDF-TrFE) copolymer. The β_a relaxation is weakened as compared with annealed samples.

tion in crystallinity and hence an increase in the fraction of the amorphous phase. Consequently, the β_a process would be expected to intensify. Quenching also generates smaller crystallites and increases the concentration of domain walls and their contribution should also enhance the β_a process. Fig. 10 compares the isothermal dielectric spectra of annealed and quenched P(VDF-TrFE) in the glass transition region. The strength of the β_a relaxation in the quenched sample is about 25% larger than that in the spectra of the annealed one, and the dielectric constant ϵ' of the former is consistently higher than that of the latter at -10°C . Similar enhancement of the β_a process for quenched P(VDF-TrFE) is also observed at other temperatures. As will be demonstrated later, quenching the ferroelectric relaxor terpolymer leads to quite different dielectric behavior, where quenching results in a reduction of both the real and imaginary dielectric constants associated with this relaxation process.

In addition to these three dielectric relaxation processes, there is a fourth relaxation occurring at lower temperatures, which is manifested as a weak shoulder on the low temperature tail of the β_a process in isochronal dielectric spectra [25–27]. This relaxation can be better presented in an isothermal plot (Fig. 11). At temperatures far below the T_g of P(VDF-TrFE) ($\sim -40^\circ\text{C}$), a clear dispersion is observed in ϵ'' . This relaxation has been denoted as the local γ process and proposed to originate from the fast rotation of the C-F bonds or motion of one monomer unit [32]. The local γ relaxation contributes an increase of 1.7 to the dielectric

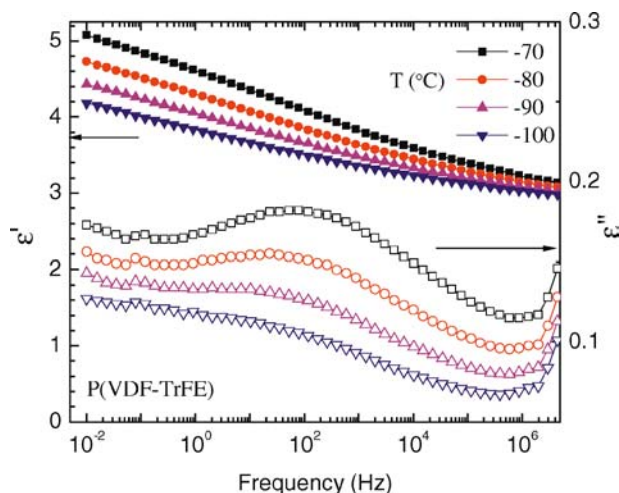


Figure 11 Isothermal dielectric spectra of P(VDF-TrFE) copolymer at low temperatures (temperatures below -70°C).

constant from 10 MHz to 0.01 Hz at -80°C . This process follows an Arrhenius law with $f_m = 1.26 \times 10^{11} \times \exp(-36.6 \text{ kJ/mol}/RT)$ (Fig. 8). The relatively low activation energy and Arrhenius behavior strongly support the non-cooperative local origin of the γ process.

3.3. Dynamics in relaxor ferroelectric P(VDF-TrFE-CFE) terpolymer

For the terpolymer investigated here, there is no sign in the dielectric spectra of an F-P transition (Fig. 12). There is no hysteresis in the dielectric data when measured in heating and in cooling. On the other hand, for terpolymers with lower CFE concentration or non-uniform CFE distribution in the terpolymer, large coherent polar-domains and a relaxor phase coexist, and a frequency-independent phase transition process is observed in both ϵ' and ϵ'' spectra, although it is shifted to lower temperatures [17]. In previous studies on high-energy electron irradiated copolymers, similar incomplete normal-relaxor conversion has also been observed in samples with insufficient irradiation treatment of the P(VDF-TrFE) copolymer [7, 8, 34]. However, increasing the irradiation dosage eliminates the ferroelectric phase in the copolymer and hence there is no sign of F-P phase transition process in the dielectric spectra in these properly treated copolymers [7].

It is interesting to note that in the same temperature range as the β_a process in the normal ferroelectric copolymer, a strong dielectric dispersion (denoted as β_r) is observed in the relaxor terpolymer, which follows the Vogel-Fulcher law Figs 12 and 13, with $f_0 = 987 \text{ MHz}$, $U = 3.86 \text{ kJ/mol} = 0.0400 \text{ eV}$, and $T_0 = 244.3 \text{ K}$. However, this relaxation process exhibits a significantly larger increase in dielectric constant ($\Delta\epsilon = \epsilon'[\text{low frequency}]$

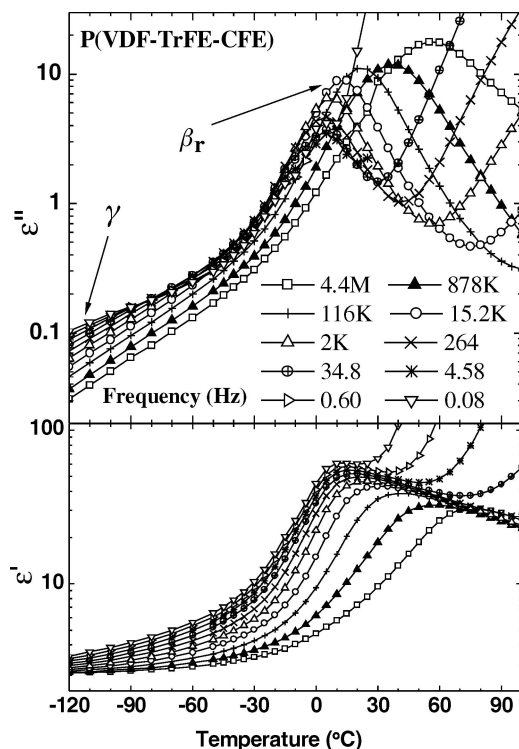


Figure 12 Dielectric spectra of P(VDF-TrFE-CFE) terpolymer at different frequencies.

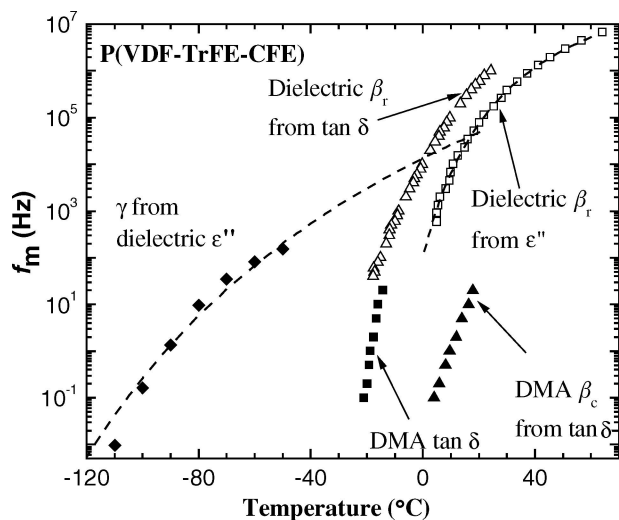


Figure 13 Relaxation times of different relaxation processes for P(VDF-TrFE-CFE) terpolymer. The γ process follows the Arrhenius equation; the linearity can be seen in the $\log f_m$ vs. $1/T$ plot. Dashed lines represent the VF - law and Arrhenius fitting to the experimental data.

$-\epsilon' = [\text{high frequency}] \frac{2}{\pi} \int_{-\infty}^{\infty} d(\ln \omega) \epsilon''(\omega)$ or $\epsilon'[\text{high temperature}] - \epsilon'[\text{low temperature}]$) and has much larger ϵ''_{max} value than β_a does. Analogous to the dielectric relaxation in the normal ferroelectric P(VDF-TrFE) copolymer, the observed β_r relaxation should include contributions from the glass transition in the amorphous phase. However, the significant increase in the dielectric constant

is a reflection of the large increase in the “domain wall” and other defects contributions of the crystalline phase. As the macroscopic polar-domains are replaced by the nano-clusters in the conversion from the normal ferroelectric to the ferroelectric relaxor, it is conceivable that there is a considerable increase in the contribution from the polar-cluster boundary motion (expanding and contracting of the nano-polar regions) and reorientation to the dielectric relaxation process. These nano-clusters have locally ordered structures; thereby their contribution to the dielectric relaxation is markedly larger than that from the completely disordered amorphous phase. This provides a direct link between the dielectric relaxation in the ferroelectric relaxor terpolymer and normal ferroelectric copolymer.

With decreasing temperature, the mobility of these nano-clusters decreases and this leads to their eventual freezing at the Vogel temperature T_0 . The relaxation time distribution for the β_r process is very broad, with peak-width at half maximum of ~ 4.4 decades at 0°C , and it becomes even broader with decreasing temperature or increasing frequency, suggesting the breakdown of the time-temperature superposition principle. This broad distribution in general reflects heterogeneity at the molecular level: for example, the presence of random defects in the crystalline phase (due to CFE), the random coupling between the local nano-clusters due to random spacing and orientation among them, lead to a distribution of dynamic cooperativity. The broadening with decreasing temperature also suggests that the intermolecular cooperativity is enhanced at lower temperatures due to the reduced fractional free volume and/or chain mobility [31]. Furthermore, this heterogeneity scenario also leads to a broad distribution in T_0 . That is, with decreasing temperature, the freezing-in occurs gradually from those processes with long relaxation times to those with short relaxation times. This is consistent with earlier studies employing a reduced dielectric constant scheme [18, 19]. It was found that the longest relaxation time follows a Vogel-Fulcher form and diverges at a freezing temperature near 0°C . The shortest relaxation time, however, exhibits Arrhenius behavior and remains active to temperatures well below -70°C . [18] Therefore, the fitting parameters (such as T_0) to the V-F law of the data in Fig. 12 are a measure of the averaged freezing process in the ferroelectric relaxor, rather than the freezing temperature T_f of the system at which the longest relaxation time in the system diverges.

The β_c process is also observed at low frequencies in the terpolymer at temperatures higher than the β_r relaxation, in both dielectric and DMA spectra Figs 12 and 14. Both processes shift to higher temperatures with increasing frequency. However, dielectric loss of the β_r relaxation, associated with segmental motion and nanocluster reorientation, is enhanced much more significantly than

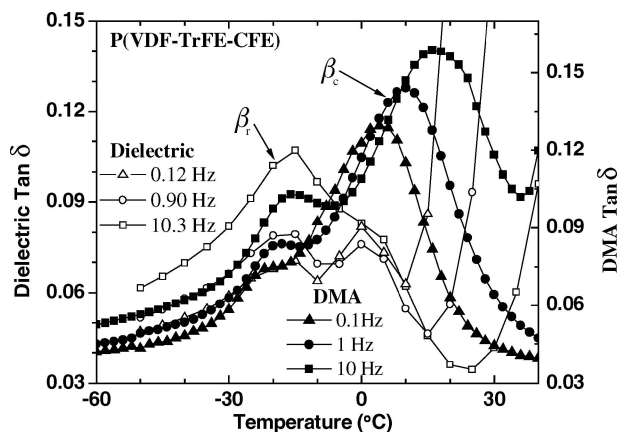


Figure 14 Comparison of the dielectric and DMA spectra of P(VDF-TrFE-CFE) terpolymer. The β_c relaxation can be clearly identified in the DMA spectra.

β_c . As a result, the latter process is completely masked by the former at higher frequencies and only one combined peak is visible in ϵ'' spectra at frequencies larger than 100 Hz.

The dielectric properties of the terpolymer were also measured after being subjected to an electric field of 100 MV/m at 50°C for 10 min, similar to the poling conditions applied to the copolymer. There is essentially no change in the dielectric β_r process before and after the application of the electric field, which is expected for the ferroelectric relaxor poled at temperatures where the slim polarization loop is observed. This supports complete conversion to the ferroelectric relaxor phase in this terpolymer.

In contrast to the behavior observed for the normal ferroelectric copolymer, quenching the relaxor ferroelectric terpolymer leads to a 50% decrease of the β_r relaxation strength in the ϵ'' spectra at 0°C and a concurrent reduction in ϵ' (Fig. 15). This result supports the notion that the β_r process in the terpolymer is not simply associated with segmental motion in the amorphous phase, which would otherwise have led to an increase in the relaxation strength. An earlier study by Klein *et al.* found that quenching P(VDF-TrFE-CFE) not only retards the crystallization process, but also induces the formation of polar *all trans* conformation, that is, reducing the content of relaxor nanoclusters [17]. Since the boundary motions and reorientation of nanoclusters dominate the β_r process, the reduction of ϵ' and ϵ'' in the quenched terpolymer is consistent with the proposed molecular origin.

Analogous to the copolymer, at temperatures significantly below T_g , the local γ relaxation is observed in the terpolymer (Figs 12 and 16). Unlike the β_r process, the γ transition exhibits Arrhenius behavior with $f_m = 1.88 \times 10^{12} \times \exp(-42.6 \text{ kJ/mol}/RT)$. When compared with the copolymer, the γ relaxation of the terpoly-

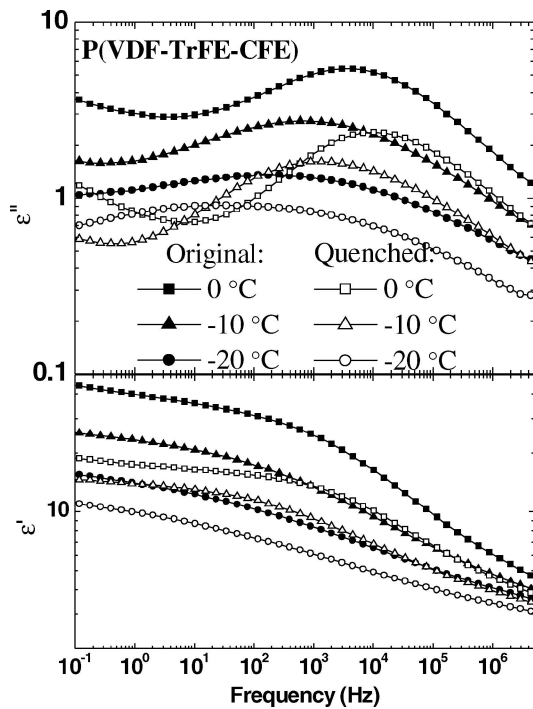


Figure 15 Isothermal dielectric spectra of quenched P(VDF-TrFE-CFE) terpolymer. The β_c relaxation is significantly weakened and sped up as compared with annealed samples.

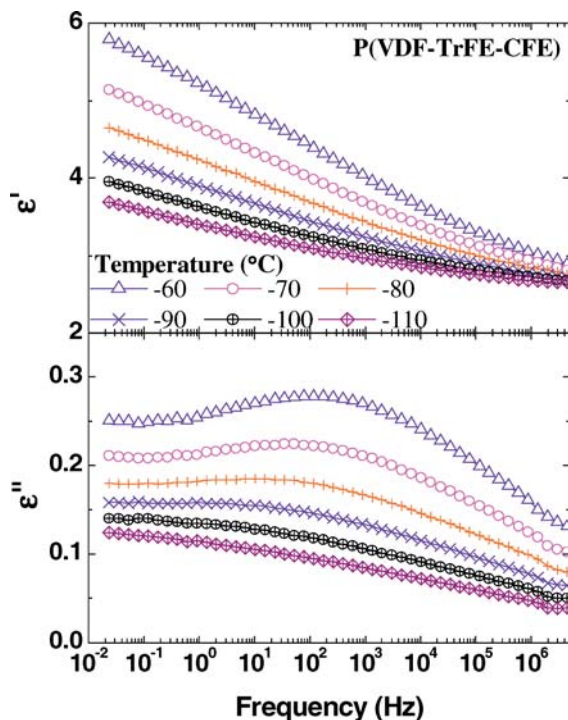


Figure 16 Isothermal dielectric spectra of P(VDF-TrFE-CFE) terpolymer at low temperatures. The dielectric constant exhibits clear step increase as a result of this relaxation.

mer is about 2 times slower and exhibits a larger activation energy. This may be due to the introduction of CFE in the polymer chain, whose bulky size may cause the local motion to become more difficult. The low temperature γ process contributes an increase of 2 to the dielectric constant at -80°C . This value much larger than that observed for the local low temperature relaxation in other common polymers with similar T_g , due to the large dipole moment of C-F [32].

4. Conclusions

In this study, we present comprehensive experimental results related to the conversion from the normal ferroelectric P(VDF-TrFE) copolymer to a relaxor ferroelectric P(VDF-TrFE-CFE) terpolymer due to the introduction of bulky CFE termonomers into the crystalline phase. Compared with the copolymer, the relaxor terpolymer exhibits high electrostrictive response and high room temperature dielectric constant. The experimental data from XRD, FTIR, DSC, and dielectric studies indicate that the macro-polar crystallites in the normal ferroelectric copolymer are transformed into a non-polar phase with local nano-clusters. There is no indication of an F-P transition in the terpolymer investigated.

The broadband dielectric spectra of both polymers exhibit rich dynamic processes, which are affected by the random introduction of the CFE in the polymer chains and by the sample treatment conditions. In the temperature range investigated (from -150 to 120°C), the copolymer exhibits at least four dielectric anomalies. The ferro-paraelectric phase transition occurs at 110°C (measured on heating). It does not depend on frequency and exhibits a large thermal hysteresis, a reflection of a first order transition process. Dynamic relaxation of polymer chains at the crystalline/amorphous interface gives rise to a weak dielectric dispersion β_c at temperatures from -20 to 40°C , depending on frequency, which is also visible in the relaxor terpolymer. The glass transition (segmental relaxation) of the amorphous phase and the domain wall relaxation in the crystalline regions, whose contributions are difficult to separate, generate a third dielectric β_a process in ϵ'' spectra, which follows the Vogel-Fulcher law. For the copolymer, quenching from the melt results in a stronger β_a relaxation due to increased domain wall density as well as an increase in the amorphous phase content. Poled samples exhibit a weaker β_a dispersion as a result of reduction of polar-defects and domain wall content in the crystalline regions under the high electric field. At temperatures below -60°C , both copolymer and terpolymer have a local dielectric γ relaxation process, which follows an Arrhenius law with an activation energy ~ 40 kJ/mol. The γ process represents polymer C - F rotation and leads to an increase of ~ 2 in dielectric constant at -80°C .

Reflecting the fact that the terpolymer P(VDF-TrFE-CFE) has been completely converted into a relaxor, no

ferro-paraelectric phase transition is observed in the dielectric spectra. The terpolymer has a β_r dielectric dispersion, in addition to β_c and γ relaxations, that is located at similar temperatures to the β_a of the copolymer. However, there is a much larger dielectric constant change associated with the β_r process compared to β_a . Combining this result with those from quenched and poled samples, as well as the behavior of the copolymer, indicates that the β_r process originates primarily from the boundary motions and reorientation of nanoclusters in the crystalline phase, similar to the dynamics observed in relaxor ferroelectric ceramics. The experimental data also reveal a broad relaxation time distribution associated with the β_r process, whose distribution width increases with reduced temperature. Fitting of the dielectric data demonstrates that the averaged relaxation time (as measured by the peak of the imaginary dielectric constant) follows the V-F law.

Acknowledgements

This work was supported by the Office of Naval Research under Grant No. N00014-02-10418 and N00014-04-10292.

References

1. H. S. NALWA, (Ed). "Ferroelectric Polymers" (Marcel Dekker, Inc. NY, 1995).
2. M. E. LINES and A. M. GLASS, "Principles and Applications of Ferroelectrics and Related Materials" (Clarendon Press, Oxford, 1977).
3. Y. BAR-COHEN, (Ed). "Electroactive Polymer (EAP) Actuators as Artificial Muscles" (SPIE, Bellingham, WA, 2001).
4. A. J. LOVINGER, *Science* **220** (1983) 1115.
5. Q. M. ZHANG, V. BHARTI and X. ZHAO, *ibid.* **280** (1998) 2101.
6. A. J. LOVINGER, D. D. DAVIS, R. E. CAIS, J. M. CAIS and J. M. KOMETANI, *Polymer* **28** (1987) 617.
7. Z. Y. CHENG, Q. M. ZHANG and F. B. BATEMAN, *J. Appl. Phys.* **92** (2002) 6749.
8. V. BHARTI, H. S. XU, G. SHANTHI, Q. M. ZHANG and K. LIANG, *ibid.* **87** (2000) 452.
9. H. S. XU, Z.-Y. CHENG, D. OLSON, M. TAI, Q. M. ZHANG and G. KAVARNOS, *Appl. Phys. Lett.* **78** (2001) 2360.
10. F. BAUER, E. FOUSSON, Q. M. ZHANG and L. M. LEE, *Proc. 11th Int. Symp. Electrets* (2002) 355.
11. F. XIA, Z. Y. CHENG, H. S. XU, H. F. LI, Q. M. ZHANG, G. J. KAVARNOS, R. Y. TING, G. ABDEL-SADEK and K. D. BELFIELD, *Adv. Mater.* **14** (2002) 1574.
12. T. C. CHUNG and A. PETCHSUK, *Macromolecules* **35** (2002) 7678.
13. C. M. ROLAND, J. T. GARRETT, R. CASALINI, D. F. ROLAND, P. G. SANTANGELO and S. B. QADRI, *Chem. Mater.* **16** (2004) 857.
14. J. T. GARRETT, C. M. ROLAND, A. PETCHSUK and T. C. CHUNG, *Appl. Phys. Lett.* **83** (2003) 1190.
15. R. J. KLEIN, J. RUNT and Q. M. ZHANG, *Macromolecules* **36** (2003) 7220.
16. R. J. KLEIN, F. XIA, Q. M. ZHANG, and F. BAUER, *J. Appl. Phys.* **97** (2005) 094105 submitted.
17. R. J. KLEIN and M. S. THESIS, The Pennsylvania State University, 2004.
18. V. BOBNAR, B. VODOPIVEC, A. LEVSTIK, M. KOSEC, B. HILCZER and Q. M. ZHANG, *Macromolecules* **36** (2003) 4436.
19. B. VODOPIVEC, V. BOBNAR, A. LEVSTIK and Q. M. ZHANG, *Ferroelectrics* **304** (2004) 857.
20. Z. YU and C. ANG, *Appl. Phys. Lett.* **84** (2004) 2145.
21. C. ANG and Z. YU, *Adv. Mater.* **16** (2004) 979.
22. Z. YU, C. ANG, L. E. CROSS, A. PETCHSUK and T. C. CHUNG, *Appl. Phys. Lett.* **84** (2004) 1737.
23. L. E. CROSS, *Ferroelectrics* **151** (1994) 305.
24. *Idem., ibid.* **76** (1987) 241.
25. T. FURUKAWA, *Phase Transitions* **18** (1989) 143.
26. T. FURUKAWA, M. OHUCHI, A. CHIBA and M. DATE, *Macromolecules* **17** (1984) 1384.
27. T. FURUKAWA, Y. TAJITSU, X. ZHANG and G. E. JOHNSON, *Ferroelectrics* **135** (1992) 401.
28. Y. ISHIDA, S. SAITO, M. ASABINA and H. KAKUTANI, *J. Polym. Sci. Part A2* **7** (1969) 1405.
29. S. YANO, *ibid., Sci. Part A2* **8** (1970) 1057.
30. K. OMOTE, H. OHIGASHI and K. KOGA, *J. Appl. Phys.* **81** (1997) 2760.
31. J. D. FERRY, "Viscoelastic Properties of Polymers" (Wiley, New York, 1980).
32. N. G. MCCRUM, B. E. READ and G. WILLIAMS, "Anelastic and Dielectric Effects in Polymeric Solids" (Wiley, London, 1967).
33. T. YAGI, M. TATEMOTO and J. SAKO, *Polym. J.* **12** (1980) 209.
34. V. BOBNAR, B. VODOPIVEC, A. LEVSTIK, Z. Y. CHENG and Q. M. ZHANG, *Phys. Rev. B* **67** (2003) 94205.